ACS chemical biology

Articles

pubs.acs.org/acschemicalbiology

# Peptide-Based Investigation of the *Escherichia coli* RNA Polymerase $\sigma^{70}$:Core Interface As Target Site

Kristina Hüsecken,[§,†] Matthias Negri,[§,†] Martina Fruth,[‡] Stefan Boettcher,[‡] Rolf W. Hartmann,[†,‡] and Joerg Haupenthal*[,†]

[†]Helmholtz Institute for Pharmaceutical Research Saarland (HIPS), Department of Drug Design and Optimization and [‡]Pharmaceutical and Medicinal Chemistry, Saarland University, Campus C2_3, D-66123 Saarbrücken, Germany

Supporting Information

**ABSTRACT:** The number of bacterial strains that are resistant against antibiotics increased dramatically during the past decades. This fact stresses the urgent need for the development of new antibacterial agents with novel modes of action targeting essential enzymes such as RNA polymerase (RNAP). Bacterial RNAP is a large multi-subunit complex consisting of a core enzyme (subunits: $\alpha_2\beta\beta'\omega$) and a dissociable sigma factor ($\sigma^{70}$; holo enzyme: $\alpha_2\beta\beta'\omega\sigma^{70}$) that is responsible for promoter recognition and transcription initiation. The interface between core RNAP and $\sigma^{70}$ represents a promising binding site. Nevertheless, detailed studies investigating its druggability are rare. Compounds binding to this region could inhibit this protein−protein interaction and thus holo enzyme formation, resulting in inhibition of transcription initiation. Sixteen peptides covering different regions of the *Escherichia coli* $\sigma^{70}$:core interface were designed; some of them−all derived from $\sigma^{70}$ 2.2 region−led to a strong RNAP inhibition. Indeed, an ELISA-based experiment confirmed the most active peptide P07 to inhibit the $\sigma^{70}$:core interaction. Furthermore, an abortive transcription assay revealed that P07 impedes transcription initiation. In order to study the mechanism of action of P07 in more detail, molecular dynamics simulations and a rational amino acid replacement study were performed, leading to the conclusion that P07 binds to the coiled-coil region in $\beta'$ and that its flexible N-terminus inhibits the enzyme by interaction with the $\beta'$ lid-rudder-system (LRS). This work revisits the $\beta'$ coiled-coil as a hot spot for the protein−protein interaction inhibition and expands it by introduction of the LRS as target site.

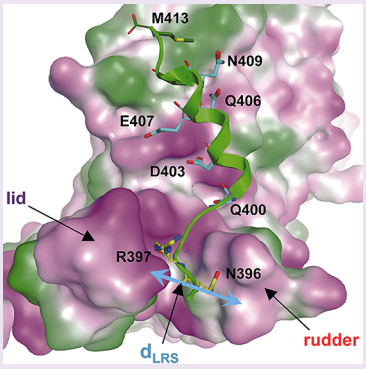


As bacterial RNA polymerase (RNAP) is essential for bacterial growth and survival, it is an attractive target for drug development.[1,2] RNAP is highly conserved among bacteria, enabling the development of broad spectrum antibiotics. Along with the recently (May 2011) FDA approved RNAP inhibitor Lipiarmycin (fidaxomicin/Dificid),[3] the Rifamycins are the only RNAP inhibitors that are in clinical use.[2] However, the use of the Rifamycins led to the occurrence of single point mutations in the *rpoB* gene (encoding for the beta subunit of the enzyme), resulting in strains that exhibit highly elevated MIC values.[4,5] Also resistance mechanisms other than target mutation have been reported for Rifampicin.[6]

Besides the Rifamycin binding site, numerous other binding sites in RNAP for diverse inhibitors are known.[7−11] In this context several new inhibitors of RNAP have been discovered in *in vitro* tests, ranging from highly active natural products[12−14] to small organic molecules.[7,8,15,16] However, these compounds also bear several disadvantages, such as poor antibacterial activity,[8] insufficient specificity for RNAP,[17] minimal absorption into mammalian cells,[18] or inadequate physicochemical properties,[19,20] which impede their use in the clinic. A strategy to overcome these drawbacks is the development of new antibacterial agents with novel and defined modes of action.

In this study we focus on the interface between the *Escherichia coli* (*E. coli* or *Ec*) RNAP core enzyme and $\sigma^{70}$ as a potential binding site in order to inhibit their assembly, which is essential for transcription initiation. As no $\sigma^{70}$ homologue has been found in mammalian cells except some specificity factors in mitochondria that seem to be more related to viral transcription systems,[21] we do not expect side effects of a drug targeting this assembly step.

We applied a peptide approach to provide a basis for the generation of new classes of RNAP inhibitors that interfere with a defined binding site within this interface. The recent identification of a peptidic RNAP inhibitor[22] and the structural studies of Sharp and colleagues[23] motivated us to rationally design a set of peptides derived from different interface regions (taken from $\beta$, $\beta'$, and $\sigma^{70}$ subunits). The peptides were chosen on the basis of mutagenesis data[23−27] and 3D information of the enzyme (e.g., PDB 3IYD).

In a transcription assay utilizing RNAP core and holo enzyme in parallel we identified two peptides with $IC_{50}$'s in the low micromolar range, both of them derived from the $\sigma^{70}$ 2.2 region. They inhibited RNAP holo enzyme more strongly than the core enzyme, supporting our idea of their mode of action. ELISA-based binding experiments confirmed the most active

**Received:** October 24, 2012
**Accepted:** January 18, 2013
**Published:** January 18, 2013

   dx.doi.org/10.1021/cb3005758 | *ACS Chem. Biol.* 2013, 8, 758−766

**Table 1. List of Designed Peptides; Details Concerning Selected Peptides Are Given**

| Peptide | Subunit[a] | Amino acid sequence[b] | Length (aa) |
|---|---|---|---|
| P01 | $\sigma^{70}$ (375-390) | AKKEMVEANLRLVISI | 16 |
| P02 | $\sigma^{70}$ (380-395) | VEANLRLVISIAKKYT | 16 |
| P03 | $\sigma^{70}$ (385-402) | RLVISIAKKYTNRGLQFL | 18 |
| P04 | $\sigma^{70}$ (385-408) | RLVISIAKKYTNRGLQFLDLIQEG | 24 |
| P05 | $\sigma^{70}$ (387-404) | VISIAKKYTNRGLQFLDL | 18 |
| P06 | $\sigma^{70}$ (390-407) | IAKKYTNRGLQFLDLIQE | 18 |
| P07 | $\sigma^{70}$ (395-413) | TNRGLQFLDLIQEGNIGLM | 19 |
| P08 | $\sigma^{70}$ (400-416) | QFLDLIQEGNIGLMKAV | 17 |
| P09 | $\sigma^{70}$ (440-457) | TRSIADQARTIRIPVHMI | 18 |
| P10 | $\sigma^{70}$ (492-507) | DKIRKVLKIAKEPISM | 16 |
| P11 | $\sigma^{70}$ (552-568) | TAREAKVLRMRFGIDMN | 17 |
| P12 | $\sigma^{70}$ (594-609) | ALRKLRHPSRSEVLRS | 16 |
| P13 | β' (265-280) | LNDLYRRVINRNNRLK | 16 |
| P14 | β' (275-290) | RNNRLKRLLDLAAPDI | 16 |
| P15 | β' (291-306) | IVRNEKRMLQEAVDAL | 16 |
| P16 | β (893-907) | TQLTPEEKLLRAIFG | 15 |
| C01[c] | - | LATKALYIERLASATA | 16 |
| C02[c] | - | RQRVEELSKFSKKGAAARRRK | 21 |
| C03[c] | - | SIGSALKKALPVAKKIGKIALPIAKAALP | 29 |
| C04[c] | - | GWGSFFKKAAHVGKHVGKAALTHYL | 25 |

[a] $\sigma^{70}$, $\beta$, and $\beta'$ subunits; in brackets: amino acid (aa) positions according to the *E. coli* RNAP subunit sequences. [b] Underlined and in red: aa that are most important for $\sigma^{70}$:core interaction, according to the literature.[23−27] P01-08 are shifted in their lines for comparability reasons. [c] Control peptides.

peptide P07 to inhibit the interaction between $\sigma^{70}$ and the core enzyme. Furthermore, an abortive transcription assay revealed that P07 impedes the initiation of transcription. Molecular dynamics (MD) simulations, which were accompanied by studies in which mutated variants of P07 were examined, suggested P07 to target the $\beta'$ coiled-coil and lid-rudder-system ($\beta'$CC-LRS) hot spot.

In this work we revisited the $\beta'$CC, which was already proposed by the group of Burgess as a promising binding site,[16,28] and expanded it by introducing the LRS as target site, resulting in a hot spot for potent inhibition of the protein−protein interaction. Our data might lead to the generation of new antibacterial drugs targeting RNAP with a novel mode of action.

## RESULTS AND DISCUSSION

**Design of Peptides.** In order to inhibit the $\sigma^{70}$:core protein−protein interaction, we designed 16 peptides derived from the most promising regions in the $\sigma^{70}$:core interface of *E. coli* RNAP. Their sequences span from 15 to 24 amino acids (aa) (Table 1). The bases for their selection were published mutagenesis data[23−27] and structural information.

In detail, 12 peptides were selected from *Ec* $\sigma^{70}$ (P01−12). We considered all aa that were reported to elicit at least 5-fold core binding defects, which were Leu384, Val387, Leu402, Asp403, Gln406, Glu407, Asn409, Met413, Pro453, Pro504, Glu555, Arg562, Ile565, and Leu598 (Table 1, aa highlighted in red).[23] Furthermore, $\sigma^{70}$ residues 361−390 (P01−06) were reported to be important for efficient core-binding activity (Table 1, underlined aa).[24] Peptides P13−15 are derived from *Ec* $\beta'_{260-309}$, a coiled-coil region ($\beta'$CC) that is reported as binding hot spot for $\sigma^{70}$.[22,25,26,29,30] Amino acid mutations R275Q, E295K, and A302D led to inviable cells in an *in vivo* assay and prevented holoenzyme formation.[25] These relevant aa are present in P13−15 (Table 1, highlighted in red). P16 represents the *Ec* $\beta$ flap-tip helix (underlined aa) and contains a hydrophobic patch described to interact with the $\sigma^{70}$ region 4.[27] Four more peptides were chosen as control peptides that should not inhibit RNAP. The aa sequence of control peptide C01 was chosen randomly, whereas C02−04 are reported to have antimicrobial activity.[31−36]

**Activity in Transcription Assay.** In order to investigate whether these peptides inhibit the $\sigma^{70}$:core interaction, transcription reactions with either core or holo RNAP were performed. We first tested the RNAP inhibitors Rifampicin, Corallopyronin, and CBR703,[6,8,13] which are described to inhibit the RNAP core enzyme, as well as Lipiarmycin (Lpm) and SB2, described to target the $\sigma^{70}$:core interaction.[7,37−39]

As our results illustrate (Table 2), the $IC_{50}$ values of the core enzyme inhibitors were around 2-fold lower for the core enzyme (compared to holo), while SB2 and Lpm inhibited the


dx.doi.org/10.1021/cb3005758 | *ACS Chem. Biol.* 2013, 8, 758−766

**Table 2. Transcription Assay with Reference Compounds and Peptides[c]**

A.

| Compound | Inhibition of RNAP core ($IC_{50}$ in μM) | Inhibition of RNAP holo ($IC_{50}$ in μM) | Ratio ($IC_{50}$ core:$holo_{compd}$ / $IC_{50}$ core:$holo_{rif}$) |
|---|---|---|---|
| Rifampicin | **0.016** | 0.027 | 1.0 |
| Corallopyronin | **0.41** | 0.65 | 1.1 |
| CBR703 | **6.5** | 13.3 | 0.9 |
| *SB2* | 56.8 | **37.9** | 2.6 |
| *Lipiarmycin* | 3.11 | **0.90** | 6.1 |

B.

| Peptide | Inhibition of RNAP core ($IC_{50}$ in μM)[a] | Inhibition of RNAP holo ($IC_{50}$ in μM)[a] | Ratio ($IC_{50}$ core:$holo_{peptide}$ / $IC_{50}$ core:$holo_{rif}$) |
|---|---|---|---|
| P01 | 40.1 | **35.3** | 2.0 |
| P02 | 24.1 | **22.9** | 1.8 |
| P03 | 15.5 % | 10.5 % | [b] |
| P04 | 9.8 | **5.8** | 3.0 |
| P05 | 21.0 % | 22.5 % | [b] |
| P06 | 21.0 % | 11.0 % | [b] |
| P07 | 6.2 | **4.6** | 2.4 |
| P08 | 25.5 % | 18.0 % | [b] |
| P09 | n.i. | n.i. | [b] |
| P10 | 10.3 % | n.i. | [b] |
| P11 | 31.4 % | 32.6 % | [b] |
| P12 | n.i. | n.i. | [b] |
| P13 | n.i. | n.i. | [b] |
| P14 | n.i. | n.i. | [b] |
| P15 | n.i. | n.i. | [b] |
| P16 | 16.0 % | n.i. | [b] |
| C01 | 42.2 | **32.2** | 2.3 |
| C02 | n.i. | n.i. | [b] |
| C03 | n.i. | n.i. | [b] |
| C04 | n.i. | n.i. | [b] |

[a]Where a % inhibition value is given, the peptide was tested at 50 μM. [b]Not determined; n.i., no inhibition (inhibition <10% at 50 μM); bold designates the lower of the two compared $IC_{50}$ values (core vs holo). Given values are in round figures; ratios are based on exact values. [c]Comparison of *Ec* RNAP inhibition (RNAP core and holo) of selected reference compounds (A) and peptides (B). $IC_{50}$ values were determined. The core to holo $IC_{50}$ ratios were related to the Rifampicin core to holo $IC_{50}$ ratios.

holo enzyme to a higher extent. On the basis of the results of these reference compounds, we expected the peptides to show a stronger inhibition of the holo enzyme.

Four out of the 16 interface-derived peptides showed >50% inhibition at 50 μM (Table 2B). Surprisingly, also the control peptide C01 showed moderate activity. As a consequence, five mutant C01 peptides were designed indicating interactions with a (still unknown) target site (Supplementary Scheme SI1).

For the most active interface-derived peptides, $IC_{50}$ values were determined. All of them inhibited the holo enzyme more strongly than core RNAP. Interestingly, the most active peptides are all derived from $\sigma^{70}$ 2.1−2.2 regions (aa 375−416; P01−08) with P07 being the most potent one with an $IC_{50}$ of 4.6 μM in the holo enzyme assay.

Although some linear peptides are known to exhibit antibacterial activity,[31−36] our peptides P01−16 did not inhibit growth of *Ec* TolC.


dx.doi.org/10.1021/cb3005758 | *ACS Chem. Biol.* 2013, 8, 758−766

**$\sigma^{70}$:core Inhibition Leads to Inhibition of Transcription Initiation.** To validate P07 inhibiting the interaction between $\sigma^{70}$ and RNAP core, we performed an ELISA-based RNAP assembly assay similar to the one published by André and colleagues.[7] In this binding experiment P07 prevented core enzyme from binding to $\sigma^{70}$ in a concentration-dependent manner, whereas P14 displayed no significant inhibition of the protein−protein interaction (Figure 1).

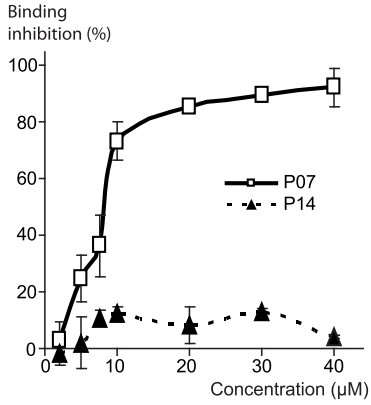


**Figure 1.** ELISA binding experiments. The binding inhibition of RNAP core to $\sigma^{70}$ is shown in the presence of different concentrations of P07 and P14. Standard deviations from two independent experiments are given (black bars).

These results support our idea for the $\sigma^{70}$:core interface region as binding site for the peptide. Nevertheless we are aware that such an effect could be also observed in the case of a conformational change within the core enzyme induced by the peptide binding to an allosteric site.

As the inhibition of $\sigma^{70}$:core interaction by P07 should inhibit promoter recognition and thus transcription initiation, an HPLC-based assay was performed aiming at the quantification of tritium-labeled abortive transcripts that are usually formed during the initiation process. As shown in Figure 2, in contrast to P14 and C03 that were inactive in the transcription assay, P07 led to a drastic reduction of abortive transcript formation, supporting again our proposed mode of action for P07.

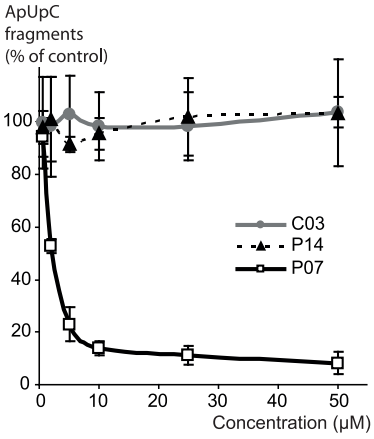


**Figure 2.** Primed abortive transcription assay. Inhibition of transcription initiation was measured by quantification of abortive transcripts (ApUpC*) that have been formed using CTP* and ApU as substrates. Asterisk (*) designates $^3$H labeling. Standard deviations from three independent experiments are given (black bars).

**MD Simulations To Elucidate Mode of Action.** In the *Thermus thermophilus* holo RNAP structure (e.g., PDB 2BE5) and in our *Ec*RNAP homology model P07 is derived from a $\sigma^{70}$ region that exhibits a helix-turn-helix motif (Figure 3A, "folding"). In order to elucidate the mechanism of action of P07 in more detail and to gain information about whether this peptide and the other peptides derived from this region (P01−08) maintain the secondary structure embodied in the holo RNAP structures, generalized Born implicit solvent simulations (100−250 ns) were carried out. The average secondary structure elements obtained are shown in Figure 3 and Supplementary Figure SI1.

While P01 and P02 almost completely maintained their helical structure during these simulations, in P03−05 only a short segment of this N-terminal helix is preserved. An explanation for the good activity of P04 could be that its rigid N-terminus is stabilized by interactions with its own apparently helical C-terminus. This was even more evident in the MD simulation of P04 in complex with a $\beta'$ truncated construct.[22] In this MD simulation, amino acids Gln400−Glu407 of P04 moved slightly toward the $\beta'$-LRS, allowing interactions of the 2.1−2.2 turn residues (Tyr394−Gln400) with lid and rudder. Shortening of P04 at both ends (P05 and P06) led to a dramatic loss of activity, possibly by losing contacts to the core enzyme and/or the LRS. P06 is identical to a peptide that was described by Sharp et al.[23] to inhibit transcription initiation, if $\sigma^{70}$ was present in unsaturated concentration. This effect was abolished if excess $\sigma^{70}$ was added to the reaction. These results emphasize the competing behavior between such a peptide and $\sigma^{70}$. In contrast to the good results for P06 in the assay performed by Sharp et al.,[23] we found only a low inhibition, presumably due to sigma saturation in the holo enzyme assay.

During the MD simulations, P07 and P08 preserved the long $\alpha$-helix seen in the holo RNAP structures for $\sigma^{70}$ 2.2. Interestingly, P07 was much more potent than P08, although the $\beta'$CC binding affinity of the latter peptide should be more efficient. On the other hand P08 lacks the five N-terminal residues (compared to P07), hinting at the N-terminal loop to be responsible for the drastic difference in activity. We speculate the LRS to be targeted by this flexible loop (instead of the rigid turn motif of P04) and decided to examine this hypothesis in more detail.

To analyze whether specific interactions are formed, GPU-accelerated MD simulations (30 ns) were performed for P07 in complex with a truncated version of $\beta'$ (aa 94−346) containing the $\beta'$CC and LRS. The absence of $\sigma^{70}$ allows an increased flexibility of the lid, which in the presence of P07 moves upward, tightening the fork formed with the rudder (distance between C$\alpha$ of Asp256 and Gly318 decreases from 23.7 to 13.8 Å) (Figure 4 and Supplementary Figure SI2). A polar network involves the $C_{term}$-core residues Gln400, Asp403, Gln406, and Glu407 and the cationic hot spot residues of $\beta'$CC Arg275, Arg278, and Arg281 (Supplementary Scheme SI2 and Supplementary Figures SI3 and SI5). In this simulation interactions can be observed between the C-terminal residues of P07 and the hydrophobic patch on the top of $\beta'$CC, which ensure an optimal placement of the peptide along the $\beta'$CC axis. As seen from the energy contribution data (Supplementary Figures SI1 and SI3), other residues strongly contributing to the binding affinity are located on the N-terminal loop of P07: Arg397 forms an ion-pair to Asp257 (lid), whereas Asn396 forms hydrogen bonds to Thr317 and Ser319 (rudder) (Figure


dx.doi.org/10.1021/cb3005758 | ACS Chem. Biol. 2013, 8, 758−766

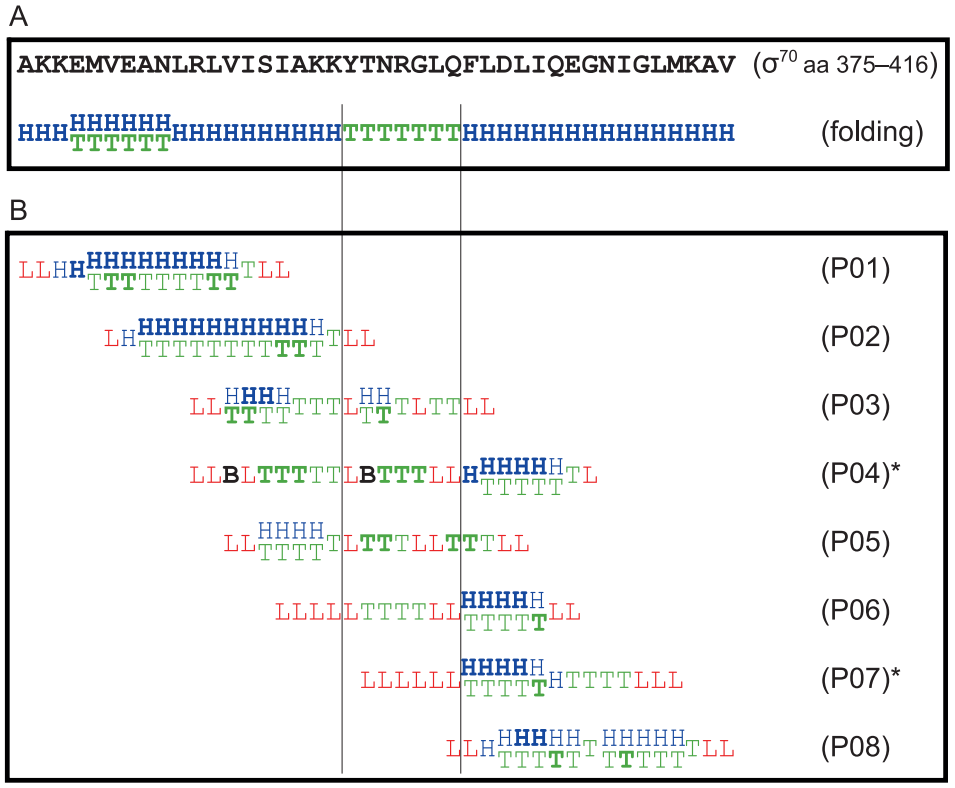


**Figure 3.** MD simulation results of P01−08. (A) The folding of the *E. coli* $\sigma^{70}$ region 375−416 is illustrated according to our *Ec* RNAP homology model. (B) The folding of each aa in P01−08 is given as a result of our MD simulations. H, helix; T, turn; L, loop; B, beta-sheet. Bold: >40% occurrence of this folding in the MD simulations; nonbold: 18−40%. Asterisk (*) designates most active peptides in the transcription assay.

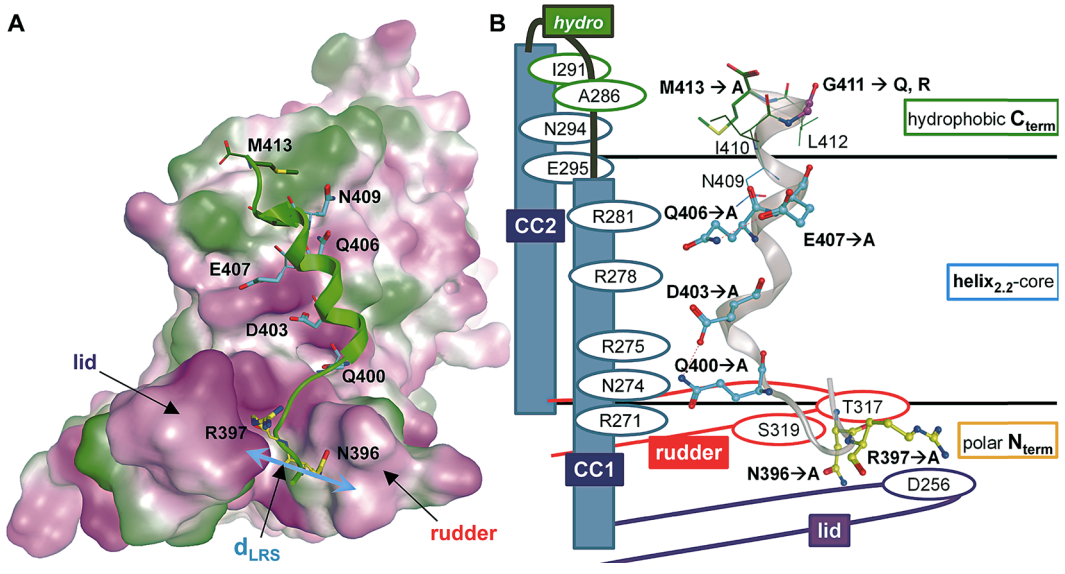


**Figure 4.** Binding of P07 to the $\beta'$trunc subunit. (A) The molecular surface representation of the $\beta'$trunc subunit (hydrophilic, magenta; neutral, white; lipophilic, dark green) is shown in complex with P07 (cartoon, green). Important residues of P07 are labeled. (B) Schematic representation of the interactions between P07 (gray cartoon) residues and the $\beta'$ coiled-coil and LRS. Residues of P07 that were varied in this study are rendered as sticks, others as lines.

4). Consequently, the LRS is stabilized in a closed conformation, which is now unavailable for $\sigma$ binding.

**Interaction Analysis by Peptide Mutants.** To confirm these hypothesized binding mechanisms and to establish a clear structure−function relationship, P07 was subjected to further *in vitro* experiments. In a first step, we designed eight mutant peptides with single-point mutations of the residues Asn396, Arg397, Gln400, Asp403, Gln406, Glu407 (all into Ala), and Gly411 (into Gln/Arg). Additionally, a truncated version of P07 lacking the six C-terminal residues was synthesized (Table 3).

The P07 mutants N396A and R397A were generated in order to prove the interactions of the N-terminal part of P07 with the LRS. Interestingly, both of these mutants showed a


dx.doi.org/10.1021/cb3005758 | *ACS Chem. Biol.* 2013, 8, 758−766

**Table 3. Transcription Inhibition by P07 Mutants[b]**

A.

| Peptide | aa sequence | Inhibition of RNAP core ($IC_{50}$ in μM) | Inhibition of RNAP holo ($IC_{50}$ in μM) | Ratio ($IC_{50}$ core:$holo_{peptide}$ / $IC_{50}$ core:$holo_{rif}$) |
|---|---|---|---|---|
| P07 | TNRGLQFLDLIQEGNIGLM | 6.2 | **4.6** | 2.4 |
| N396A | T**A**RGLQFLDLIQEGNIGLM | 35.3 | **21.0** | 2.9 |
| R397A | TN**A**GLQFLDLIQEGNIGLM | 39.4 | **18.8** | 3.7 |

B.

| Peptide | aa sequence | Inhibition of RNAP core ($IC_{50}$ in μM) | Inhibition of RNAP holo ($IC_{50}$ in μM) | Ratio ($IC_{50}$ core:$holo_{peptide}$ / $IC_{50}$ core:$holo_{rif}$) |
|---|---|---|---|---|
| P07 | TNRGLQFLDLIQEGNIGLM | 6.2 | **4.6** | 2.4 |
| Q400A | TNRGL**A**FLDLIQEGNIGLM | 11.7 | **8.0** | 2.6 |
| D403A | TNRGLQFL**A**LIQEGNIGLM | >50 | **>50** | n.d. |
| Q406A | TNRGLQFLDLI**A**EGNIGLM | 18.6 | **8.3** | 3.9 |
| E407A | TNRGLQFLDLIQ**A**GNIGLM | 17.2 | **16.3** | 1.9 |

C.

| Peptide | aa sequence | Inhibition of RNAP core ($IC_{50}$ in μM) | Inhibition of RNAP holo ($IC_{50}$ in μM) | Ratio ($IC_{50}$ core:$holo_{peptide}$ / $IC_{50}$ core:$holo_{rif}$) |
|---|---|---|---|---|
| P07 | TNRGLQFLDLIQEGNIGLM | 6.2 | **4.6** | 2.4 |
| G411Q | TNRGLQFLDLIQEGNI**Q**LM | 9.3 | **4.5** | 3.6 |
| G411R | TNRGLQFLDLIQEGNI**R**LM | 44.1 | **31.0** | 2.5 |
| 395-407[a] | TNRGLQFLDLIQE | 31.9 | **26.0** | 2.2 |

[a]Short version of P07 (aa positions referring to *E. coli* $\sigma^{70}$). n.d., not determined. [b]Selected aa of P07 were substituted (underlined). Modifications were performed in the (A) $N_{term}$ loop region, (B) $helix_{2.2}$ core, and (C) hydrophobic $C_{term}$. $IC_{50}$ values (inhibition of core and holo RNAP) were determined for these peptides.

significant loss of activity (Table 3A), confirming the MD predictions.

The four mutated residues of the $helix_{2.2}$-core (Gln400, Asp403, Gln406, Glu407) are regarded as key amino acids: they exhibited the highest binding energy contributions in the P07-$\beta'$CC-LRS MD simulation due to interactions with Arg275, Arg278, Arg281, and Glu295 (Figure 4B, Supplementary Figure SI3 and Supplementary Scheme SI2). Indeed, our *in vitro* results show a significant increase of the $IC_{50}$ values confirming the modeling results. Especially substitution D403A led to a more than 10-fold increase of the $IC_{50}$ value compared to that of P07 (Table 3B).

Finally, we examined the C-terminal part of P07 and its interactions with the hydrophobic patch at the tip of the $\beta'$CC by mutating Gly411 to Arg and Gln (Table 3C). In particular, we speculated that a neutral glutamine stabilizes the helical structure of the peptide, whereas for G411R a decreased helix stability and, notably, a repulsion with the $\beta'$CC cationic hot spot residues Arg278 and Arg281 was expected. Indeed, while the $IC_{50}$ of G411Q was similar to that of P07, the $IC_{50}$ of G411R increased around 7-fold (Table 3C). As expected a truncated version of P07 lacking the six C-terminal aa exhibits a reduced activity (26 μM, Table 3C), suggesting that it might still target $\beta'_{trunc}$.

To further investigate the roles of the peptides D403A, G411Q, and G411R, they were simulated alone as well as in complex with the truncated $\beta'$ construct. The helical structure of D403A was not altered compared to P07, but in contrast to P07, which is oriented parallel to the $\beta'$CC-axis with closed LRS, in the D403A-$\beta'_{trunc}$ simulation D403A is rotated perpendicularly along the $\beta'$CC axis (Figure 5).

The lack of interactions with lid or rudder leads to an opened LRS conformation ($d_{LRS}$ = 22.6 Å), which is likely accessible for $\sigma$. The decreased predicted binding energy is in agreement with the reduced inhibition, the energy contribution data (Supplementary Figure SI3), and the hydrogen bonds (Supplementary Scheme SI2). Notably, for the G411Q complex the peptide is oriented along the $\beta'$CC axis as seen for P07 with its N-terminal loop fitted in between a closed LRS ($d_{LRS}$ = 13.2 Å) (Figure 5B and Supplementary Figure SI2). Moreover, for this complex the binding energy was in agreement with the inhibitory potency. For the G411R-$\beta'_{trunc}$ simulation the ion-pair network formed by Asp403 with Arg275 and Arg278 is maintained holding the $helix_{2.2}$ core in place. However, it is


dx.doi.org/10.1021/cb3005758 | *ACS Chem. Biol.* 2013, 8, 758−766

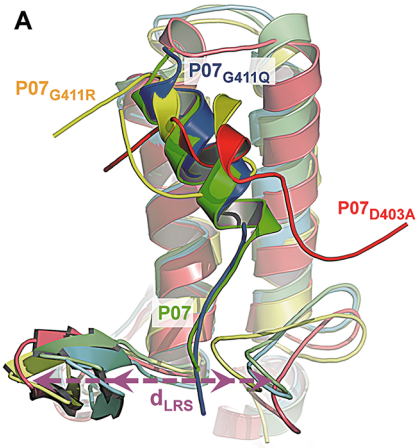


B

| peptide | $d_{LRS}$ (Å) | $\Delta G_{bind}$ | $IC_{50}$ (μM) |
|---|---|---|---|
| P07 | 13.8 | -55.69 | 4.6 |
| D403A | 22.6 | -37.00 | >50 |
| G411Q | 13.2 | -59.93 | 4.5 |
| G411R | 21.5 | -41.57 | 31.0 |

**Figure 5.** Binding of P07 and selected mutants to the $\beta'$trunc subunit. (A) Superimposition of the simulated peptides-$\beta'$trunc complexes: P07 (green), D403A (red), G411Q (blue), G411R (yellow). (B) The shorter $d_{LRS}$ values for P07 and G411Q correlate with more favorable $\Delta G_{bind}$ and $IC_{50}$ values.

rotated with respect to the $\beta'$CC axis (as seen for D403A). Arg411 is pulled away from the $\beta'$ hydrophobic patch, leading to unfolding of the C-terminal helix. Along with the observation that the LRS is found in an opened conformation, these data explain the reduced RNAP inhibition by G411R. Accordingly, our MD-based hypothesis for the mechanism of action of P07 are consistent with our *in vitro* data.

**Conclusions.** In the present work we examined rationally designed peptides as inhibitors of $\sigma^{70}$:core interaction. We focused on peptide P07, which showed the best inhibitory activity. ELISA-based binding experiments as well as successful inhibition of transcription initiation by P07 strongly support the $\sigma^{70}$:core interface as a target site. After performing MD simulations and detailed mutagenesis studies, we conclude that P07 binds to the $\beta'$CC and to the LRS. Our results indicate that both interaction sites are essential for potent inhibition. Notably, P07 also led to a significant inhibition of the RNAP core enzyme. Although this result is at a first glance surprising, an explanation is found in the MD simulations and the mutagenesis results. In particular, interference of P07 with the conformational flexibility of the LRS might be the cause for the observed core RNAP inhibition. This hypothesis is supported by the fact that mutagenesis and deletion experiments of lid[40] and/or rudder[41,42] affected the initiation step (as expected for pure sigma-core inhibitors), but also other transcription events such as open promoter complex formation and RNA exit. These data might be used as a valuable starting point for the structure-based design of small organic molecules addressing this target site.

## METHODS

**Transcription Assay.** Core and holo enzyme of *E. coli* RNA polymerase were purchased from Epicenter Biotechnologies. Final concentrations in a total volume of 30 μL were 20 units of RNase inhibitor (RiboLock, Fermentas), 10 mM DTT, 40 mM Tris HCl (pH 7.5), 150 mM KCl, 10 mM $MgCl_2$, 0.01% (v/v) Triton-X-100, 400 μM ATP, CTP, and GTP, as well as 100 μM UTP. As enzymes and for detection, 1 unit of RNAP holo enzyme was used along with 0.53 μM $^3$H-UTP and 1 unit of RNAP core enzyme was used along with 1.33 μM $^3$H-UTP. As template for the transcription reactions 425 ng of T7A1 (for holo) or T7 (for core) promoter containing PCR fragments served as templates, respectively. Prior to starting the experiment, the compounds were dissolved in DMSO, and the peptides were dissolved in a 1:1 mixture of acetonitrile (ACN) and $ddH_2O$. The final DMSO concentration during the experiments was 2% (v/v) (1% (v/v) for ACN). Dilution series of compounds were prepared using a liquid handling system (Janus, Perkin-Elmer). Further steps including the preincubation, transcription reaction, purification, and quantification were performed as described previously.[43] To obtain inhibition values for each sample, their counts were related to DMSO or ACN/$ddH_2O$ controls, respectively.

**Preparation of DNA Templates.** To obtain the T7A1 template, a two-step PCR was performed using Taq DNA polymerase (New England Biolabs). First, a part of the neomycin gene of pcDNA3.1 was amplified. The 3′ primer (ttctcggcaggagcaaggtgag) was used along with a 5′ oligo which was flanked by a T7A1 promoter (gactcagtgatatcaaaaagagtattgacttaaagtctaacctataggatacttacagccatcgagaggctgatcaagagacaggatgagg) resulting in a PCR product containing the 59-bp T7A1 promoter on the 5′ end. The total size of the PCR product was 437 bp. To obtain the T7 promoter template the same procedure as above was followed with the difference that the T7A1 promoter sequence was substituted by the T7 promoter sequence. The PCR products were gel purified (kit from PEQLAB) and elongated in a second PCR using the same 3′ oligos and a 5′ oligo increasing the size by 13 bp (cagaccatgatcagactcagtgatatc). The PCR products were purified (kit from Fermentas) and served as templates in our transcription assays.

**Determination of $IC_{50}$ Values.** Three different concentrations of a compound/peptide were chosen for the determination of an $IC_{50}$ value (two samples for each concentration). The calculation of the $IC_{50}$ value was performed by plotting the percent inhibition versus the concentration of inhibitor on a semilog plot. From this the molar concentration causing 50% inhibition was calculated. At least three independent determinations were performed for each compound.

**RNA Polymerase Inhibitors and Peptides That Were Used.** Rifamycin was purchased from Sigma-Aldrich. Corallopyronin was donated by K. Gerth (HZI). CBR703 (benzenecarboximidamide, *N*-hydroxy-*N*′-phenyl-3-(trifluoromethyl)) was synthesized according to a published procedure (WO 01/51456 A2). SB2 (benzoic acid, 3-[5-[[4-oxo-3-(2-propen-1-yl)-2-thioxo-5-thiazolidinylidene]methyl]-2-furanyl]) was synthesized as described in the literature.[44] Lipiarmycin was a generous gift from Novartis. Peptides were purchased from intavis, peptides&elephants, or were synthesized by our *in house* Platform Peptide Synthesis. Peptide sequences are given in Table 1.

**ELISA Experiments.** The procedure was performed as described in André et al.[7] with slight modifications regarding quantification. The cloning and purification of *Ec* $\sigma^{70}$ was performed as described in Haupenthal et al.[43] As primary antibody for the detection of core enzyme binding, a monoclonal anti-α subunit antibody was purchased from NeoClone Biotechnology. This antibody was used in a 1:1000 dilution as recommended by the manufacturer. The secondary antibody, a goat anti-mouse IgG labeled with fluorescein (Santa Cruz Biotechnology) was used diluted 1:200. Fluorescein was excited at 485 nm, and fluorescence read out at 520 nm on a microplate reader (POLARstar Omega by BMG Labtech).

**HPLC-Based Abortive Transcription Assay.** *E. coli* RNA polymerase (RNAP) holo enzyme was purchased from Epicenter Biotechnologies. Final concentrations in a total volume of 30 μL were 1 unit of RNAP along with 20 units of RNase inhibitor (RiboLock, Fermentas), 10 mM DTT, 40 mM Tris-HCl (pH 7.5), 150 mM KCl, 10 mM $MgCl_2$, and 0.1% (w/v) CHAPS. The peptides were dissolved in a 1:1 mixture of acetonitril (ACN) and water (final ACN concentration during experiments: 1% (v/v)). In the presence of the above-mentioned RNAP mixture they were incubated for 10 min at 25 °C prior to starting the experiment. Each transcription reaction was started by the addition of a mixture containing 1 μCi of [5-$^3$H]-CTP (Perkin-Elmer), 100 μM of ApU dinucleotide (IBA), and 450 ng of the T7A1 promoter containing PCR product T7A1_437 serving as the


dx.doi.org/10.1021/cb3005758 | ACS Chem. Biol. 2013, 8, 758−766

DNA template.[43] The transcription reactions were carried out at 37 °C for 60 min. The subsequent sample preparation and HPLC-based quantification of ApUpC formation were carried out as described in the Supporting Information.

**Molecular Dynamics (MD) Simulations, MM-GBSA Calculations, and Minimal Inhibitory Concentration (MIC) Determinations.** The description of these methods can be found in the Supporting Information.

## ■ ASSOCIATED CONTENT

### Supporting Information

This material is available free of charge *via* the Internet at http://pubs.acs.org.

## ■ AUTHOR INFORMATION


### Corresponding Author

*E-mail: jha09@helmholtz-hzi.de.


### Author Contributions

§These authors contributed equally to this work. All authors have given approval to the final version of the manuscript.

### Notes

The authors declare no competing financial interest.

## ■ ACKNOWLEDGMENTS

We thank E. Schmitt (Novartis) for providing Lipiarmycin and K. Gerth (HZI) for supplying us with Corallopyronin. Also we thank J. Jung for excellent technical support as well as J. C. de Jong for synthesizing CBR703 and SB2.

## ■ REFERENCES


(1) Chopra, I. (2007) Bacterial RNA polymerase: a promising target for the discovery of new antimicrobial agents. *Curr. Opin. Invest. Drugs 8*, 600−607.

(2) Mariani, R., and Maffioli, S.-I. (2009) Bacterial RNA polymerase inhibitors: an organized overview of their structure, derivatives, biological activity and current clinical development status. *Curr. Med. Chem. 16*, 430−454.

(3) Talpaert, M., Campagnari, F., and Clerici, L. (1975) Lipiarmycin: an antibiotic inhibiting nucleic acid polymerases. *Biochem. Biophys. Res. Commun. 63*, 328−334.

(4) Bryskier, A. (2005) Anti-MRSA agents: under investigation, in the exploratory phase and clinically available. *Expert Rev. Anti-Infect. Ther. 3*, 505−553.

(5) Floss, H.-G., and Yu, T.-W. (2005) Rifamycin-mode of action, resistance, and biosynthesis. *Chem. Rev. 105*, 621−632.

(6) Tupin, A., Gualtieri, M., Roquet-Banères, F., Morichaud, Z., Brodolin, K., and Leonetti, J.-P. (2010) Resistance to rifampicin: at the crossroads between ecological, genomic and medical concerns. *Int. J. Antimicrob. Agents 35*, 519−523.

(7) André, E., Bastide, L., Villain-Guillot, P., Latouche, J., Rouby, J., and Leonetti, J.-P. (2004) A multiwell assay to isolate compounds inhibiting the assembly of the prokaryotic RNA polymerase. *Assay Drug Dev. Technol. 2*, 629−635.

(8) Artsimovitch, I., Chu, C., Lynch, A.-S., and Landick, R. (2003) A new class of bacterial RNA polymerase inhibitor affects nucleotide addition. *Science 302*, 650−654.

(9) Mukhopadhyay, J., Sineva, E., Knight, J., Levy, R.-M., and Ebright, R.-H. (2004) Antibacterial peptide microcin J25 inhibits transcription by binding within and obstructing the RNA polymerase secondary channel. *Mol. Cell 14*, 739−751.

(10) Mukhopadhyay, J., Das, K., Ismail, S., Koppstein, D., Jang, M., Hudson, B., Sarafianos, S., Tuske, S., Patel, J., Jansen, R., Irschik, H., Arnold, E., and Ebright, R.-H. (2008) The RNA polymerase "switch region" is a target for inhibitors. *Cell 135*, 295−307.

(11) Temiakov, D., Zenkin, N., Vassylyeva, M.-N., Perederina, A., Tahirov, T.-H., Kashkina, E., Savkina, M., Zorov, S., Nikiforov, V., Igarashi, N., Matsugaki, N., Wakatsuki, S., Severinov, K., and Vassylyev, D.-G. (2005) Structural basis of transcription inhibition by antibiotic streptolydigin. *Mol. Cell 19*, 655−666.

(12) Irschik, H., Gerth, K., Höfle, G., Kohl, W., and Reichenbach, H. (1983) The myxopyronins, new inhibitors of bacterial RNA synthesis from Myxococcus fulvus (Myxobacterales). *J. Antibiot. (Tokyo) 36*, 1651−1658.

(13) Irschik, H., Jansen, R., Höfle, G., Gerth, K., and Reichenbach, H. (1985) The corallopyronins, new inhibitors of bacterial RNA synthesis from Myxobacteria. *J. Antibiot. (Tokyo) 38*, 145−152.

(14) Irschik, H., Jansen, R., Gerth, K., Höfle, G., and Reichenbach, H. (1987) The sorangicins, novel and powerful inhibitors of eubacterial RNA polymerase isolated from myxobacteria. *J. Antibiot. (Tokyo) 40*, 7−13.

(15) Arhin, F., Bélanger, O., Ciblat, S., Dehbi, M., Delorme, D., Dietrich, E., Dixit, D., Lafontaine, Y., Lehoux, D., Liu, J., McKay, G.-A., Moeck, G., Reddy, R., Rose, Y., Srikumar, R., Tanaka, K.-S., Williams, D.-M., Gros, P., Pelletier, J., Parr, T.-R., Jr., and Far, A.-R. (2006) A new class of small molecule RNA polymerase inhibitors with activity against rifampicin-resistant Staphylococcus aureus. *Bioorg. Med. Chem. 14*, 5812−5832.

(16) Glaser, B.-T., Bergendahl, V., Thompson, N.-E., Olson, B., and Burgess, R.-R. (2007) LRET-based HTS of a small-compound library for inhibitors of bacterial RNA polymerase. *Assay Drug Dev. Technol. 5*, 759−768.

(17) Mariner, K.-R., Trowbridge, R., Agarwal, A.-K., Miller, K., O'Neill, A.-J., Fishwick, C.-W., and Chopra, I. (2010) Furanyl-rhodanines are unattractive drug candidates for development as inhibitors of bacterial RNA polymerase. *Antimicrob. Agents Chemother. 54*, 4506−4509.

(18) Louie, T., Miller, M., Donskey, C., Mullane, K., and Goldstein, E.-J. (2009) Clinical outcomes, safety, and pharmacokinetics of OPT-80 in a phase 2 trial with patients with Clostridium difficile infection. *Antimicrob. Agents Chemother. 53*, 223−228.

(19) Haebich, D., and von Nussbaum, F. (2009) Lost in transcription−inhibition of RNA polymerase. *Angew. Chem., Int. Ed. 48*, 3397−3400.

(20) O'Shea, R., and Moser, H.-E. (2008) Physicochemical properties of antibacterial compounds: implications for drug discovery. *J. Med. Chem. 51*, 2871−2878.

(21) Tracy, R.-L., and Stern, D.-B. (1995) Mitochondrial transcription initiation: promoter structures and RNA polymerases. *Curr. Genet. 28*, 205−216.

(22) Negri, M., Haupenthal, J., Hartmann, R.-W. "From-macro-to-micro": dissecting bacterial RNA polymerase into druggable subdomains. (Helmholtz Institute for Pharmaceutical Research Saarland, Department of Drug Design and Optimization, Saarbrücken, Germany). Unpublished data.

(23) Sharp, M.-M., Chan, C.-L., Lu, C.-Z., Marr, M.-T., Nechaev, S., Merritt, E.-W., Severinov, K., Roberts, J.-W., and Gross, C.-A. (1999) The interface of sigma with core RNA polymerase is extensive, conserved, and functionally specialized. *Genes Dev. 13*, 3015−3026.

(24) Lesley, S.-A., and Burgess, R.-R. (1989) Characterization of the Escherichia coli transcription factor sigma 70: localization of a region involved in the interaction with core RNA polymerase. *Biochemistry 28*, 7728−7734.

(25) Arthur, T.-M., Anthony, L.-C., and Burgess, R.-R. (2000) Mutational analysis of beta'260−309, a sigma 70 binding site located on Escherichia coli core RNA polymerase. *J. Biol. Chem. 275*, 23113−23119.

(26) Zhang, G., Campbell, E.-A., Minakhin, L., Richter, C., Severinov, K., and Darst, S.-A. (1999) Crystal structure of Thermus aquaticus core RNA polymerase at 3.3 A resolution. *Cell 98*, 811−824.

(27) Geszvain, K., Gruber, T.-M., Mooney, R.-A., Gross, C.-A., and Landick, R. (2004) A hydrophobic patch on the flap-tip helix of E. coli RNA polymerase mediates sigma(70) region 4 function. *J. Mol. Biol. 343*, 569−587.

(28) Bergendahl, V., Heyduk, T., and Burgess, R.-R. (2003) Luminescence resonance energy transfer-based high-throughput

screening assay for inhibitors of essential protein-protein interactions in bacterial RNA polymerase. *Appl. Environ. Microbiol. 69*, 1492−1498.
(29) Arthur, T.-M., and Burgess, R.-R. (1998) Localization of a sigma70 binding site on the N terminus of the Escherichia coli RNA polymerase beta' subunit. *J. Biol. Chem. 273*, 31381−31387.
(30) Burgess, R.-R., and Anthony, L. (2001) How sigma docks to RNA polymerase and what sigma does. *Curr. Opin. Microbiol. 4*, 126−131.
(31) Cole, A.-M., Weis, P., and Diamond, G. (1997) Isolation and characterization of pleurocidin, an antimicrobial peptide in the skin secretions of winter flounder. *J. Biol. Chem. 272*, 12008−12013.
(32) Sung, W.-S., and Lee, D.-G. (2008) Pleurocidin-derived antifungal peptides with selective membrane-disruption effect. *Biochem. Biophys. Res. Commun. 369*, 858−861.
(33) Park, C.-B., Lee, J.-H., Park, I.-Y., Kim, M.-S., and Kim, S.-C. (1997) A novel antimicrobial peptide from the loach *Misgurnus anguillicaudatus*. *FEBS Letters 411*, 173−178.
(34) Cruciani, R.-A., Barker, J.-L., Durell, S.-R., Raghunathan, G., Guy, H.-R., Zasloff, M., and Stanley, E.-F. (1992) Magainin 2, a natural antibiotic from frog skin, forms ion channels in lipid bilayer membranes. *Eur. J. Pharmacol. 226*, 287−296.
(35) Oren, Z., and Shai, Y. (1996) A class of highly potent antibacterial peptides derived from pardaxin, a pore-forming peptide isolated from Moses sole fish Pardachirus marmoratus. *Eur. J. Biochem. 237*, 303−310.
(36) Marchini, D., Giordano, P.-C., Amons, R., Bernini, L.-F., and Dallai, R. (1993) Purification and primary structure of ceratotoxin A and B, two antibacterial peptides from the female reproductive accessory glands of the medfly *Ceratitis capitata* (Insecta: Diptera). *Insect Biochem. Mol. Biol. 23*, 591−598.
(37) Tupin, A., Gualtieri, M., Leonetti, J.-P., and Brodolin, K. (2010) The transcription inhibitor lipiarmycin blocks DNA fitting into the RNA polymerase catalytic site. *EMBO J. 29*, 2527−2537.
(38) Sonenshein, A.-L., Alexander, H.-B., Rothstein, D.-M., and Fisher, S.-H. (1977) Lipiarmycin-resistant ribonucleic acid polymerase mutants of Bacillus subtilis. *J. Bacteriol. 132*, 73−79.
(39) André, E., Bastide, L., Michaux-Charachon, S., Gouby, A., Villain-Guillot, P., Latouche, J., Bouchet, A., Gualtiéri, M., and Leonetti, J.-P. (2006) Novel synthetic molecules targeting the bacterial RNA polymerase assembly. *J. Antimicrob. Chemother. 57*, 245−251.
(40) Naryshkina, T., Kuznedelov, K., and Severinov, K. (2006) The role of the largest RNA polymerase subunit lid element in preventing the formation of extended RNA-DNA hybrid. *J. Mol. Biol. 361*, 634−643.
(41) Kuznedelov, K., Korzheva, N., Mustaev, A., and Severinov, K. (2002) Structure-based analysis of RNA polymerase function: the largest subunit's rudder contributes critically to elongation complex stability and is not involved in the maintenance of RNA-DNA hybrid length. *EMBO J. 21*, 1369−1378.
(42) Toulokhonov, I., and Landick, R. (2006) The role of the lid element in transcription by E. coli RNA polymerase. *J. Mol. Biol. 361*, 644−658.
(43) Haupenthal, J., Hüsecken, K., Negri, M., Maurer, C.-K., and Hartmann, R.-W. (2012) Influence of DNA template choice on transcription and inhibition of E. coli RNA polymerase. *Antimicrob. Agents Chemother. 56*, 4536−4539.
(44) Villain-Guillot, P., Gualtieri, M., Bastide, L., Roquet, F., Martinez, J., Amblard, M., Pugniere, M., and Leonetti, J.-P. (2007) Structure-activity relationships of phenyl-furanyl-rhodanines as inhibitors of RNA polymerase with antibacterial activity on biofilms. *J. Med. Chem. 50*, 4195−4204.